



## **BROADBAND FREQUENCY ASPERITY PARAMETERS OF CRUSTAL EARTHQUAKES FROM INVERSION OF NEAR-FAULT GROUND MOTION**

**Nelson PULIDO<sup>1</sup>**

### **SUMMARY**

Kinematic models of the source in the last decade have largely improved our understanding about the source rupture process and near-fault ground motion characteristics. However most of these models have been developed within a low frequency range (less than 1Hz). In order to be able to understand the actual damage potential of ground motion during a strong earthquake, it is necessary to investigate the source rupture characteristics and subsequent ground motion in a broader frequency range.

For that purpose we investigated a broadband source asperity model of the 2000 Tottori earthquake (Japan) and 1999 Izmit earthquake (Turkey), by applying a Genetic Algorithm (GA) inversion scheme that optimise the fitting between simulated and observed RMS acceleration envelopes of near-fault ground motion. Additionally the simulated waveforms were constrained to fit the acceleration response spectra of the observed records. The asperity location, area and seismic moment are constrained by using the available slip distributions obtained from kinematic inversions of near-fault ground motion. The calculation of broadband frequency strong ground motion (0.1 to 10Hz) is achieved by applying a hybrid technique that combines a deterministic simulation of the wave propagation for the low frequencies and a semi-stochastic modelling approach for the high frequencies. For the simulation of the high frequencies we use a frequency-dependent, subfault-site specific radiation pattern model, that efficiently removes the dependence of the pattern coefficient on the azimuth and take-off angle as the frequency increases.

The methodology presented in this paper has the flexibility to be applied for the simulation of near-fault ground motion for future (scenario) earthquakes.

### **INTRODUCTION**

Recently hybrid techniques have been proposed to calculate a broadband frequency ground motion in the near fault region. The hybrid technique, first proposed by Kamae et al. [1,2], combined a deterministic modelling of the low frequencies with the high frequency stochastic approach of Boore [3], and the convolution technique of Irikura [4] to obtain the ground motion from a heterogeneous finite fault model. These models have been widely applied to simulate the broadband near-fault ground motion for recent destructive eathquakes (Kamae et al. [2], Pitarka et. al. [5]).

---

<sup>1</sup> Researcher, National Research Institute for Earth Science and Disaster Prevention, Earthquake Disaster Mitigation Research Center, Japan. Email: nelson@edm.bosai.go.jp

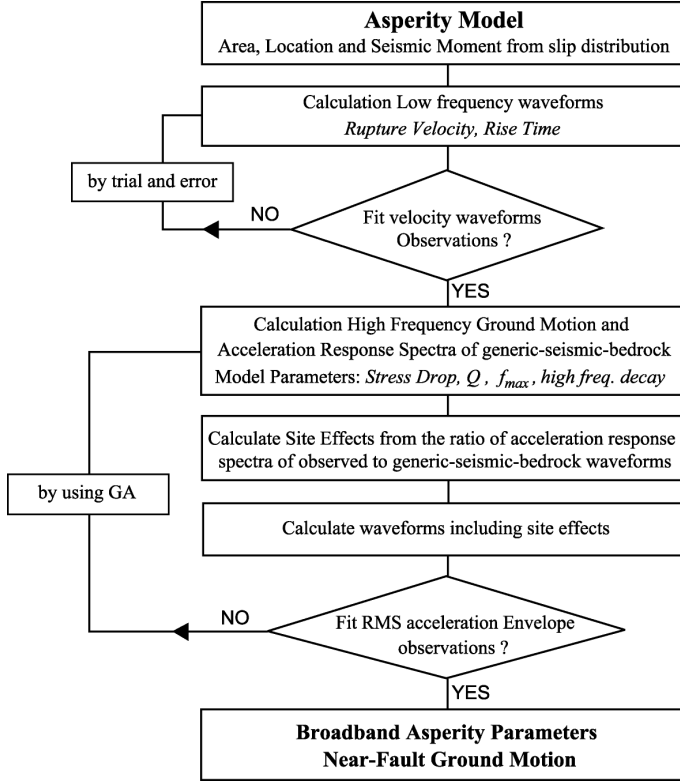


**Figure 1. Flow chart diagram for the estimation of the broadband frequency asperity parameters**

However in most of these studies, the estimation of the asperity parameters used for the forward calculation of ground motion has not been systematic, and therefore the comparison between simulated and observed broadband frequency ground motion has been very subjective.

In this study I performed a systematic search for the optimum asperity and high frequency attenuation parameters (asperity and background stress drops,  $Q(f)$ ,  $f_{max}$ , and high frequency decay), by applying a non-linear inversion scheme that optimise the fitting between observed and simulated root mean square acceleration envelopes of near-fault ground motions.

### GROUND MOTION ESTIMATION METHODOLOGY

I estimate the broadband frequency (0.1Hz to 10 Hz) near fault ground motion from a multi-asperity source model by using a hybrid technique that incorporates a frequency-dependent subfault-receiver specific radiation pattern model (Pulido et al. [6]).

#### Low frequency ground motion

I calculate the low frequency ground motion (0.1 to 1.0Hz) by applying a constant rupture velocity to a set of point sources within the fault plane. The point source ground motions are obtained by the Discrete Wave Number method of Bouchon [7] by using a smooth ramp moment function:

$$M(t) = \frac{M_0}{2} * \left( 1 + \tanh\left(\frac{4*(t - \tau/2)}{\tau}\right) \right) \quad (1)$$

where  $M_0$  is the point source seismic moment,  $t$  is the rupture time, and  $\tau$  is the asperity rise time.

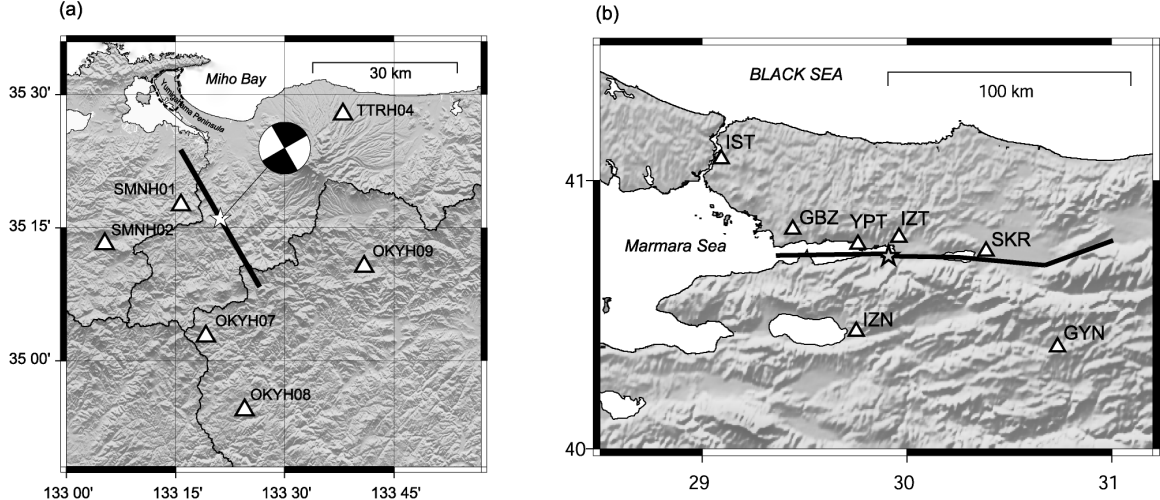


**Figure 2. (a) KiK-Net stations used for the inversion of broadband asperity parameters of the 2000 Tottori earthquake (Japan). (b) The same for the 1999 Kocaeli (Turkey) earthquake**

### High Frequency Ground Motion

High frequency ground motion (1 to 10 Hz) is calculated from a multi-asperity model as before. The point source ground motions are obtained from the stochastic approach of Boore [3], by including a frequency-dependent asperity-site specific radiation pattern coefficient  $R_{pi}(\phi_s, \delta, \lambda, \theta, \phi, f)$ , in order to account for the effect of the pattern on intermediate frequency ground motions (1 to 3 Hz) (Pulido et al. [6]). The point sources are convolved by using the procedure of Irikura [4] to obtain the multi-asperity ground motion. The  $i$  component of acceleration Fourier spectra for a point source is obtained as follows:

$$A_i(f) = \frac{R_{pi}(\phi_s, \delta, \lambda, \theta, \phi, f) M_0 S(f, f_c) F_s G(f) e^{-\pi R/Q(f)\beta}}{4\pi\rho\beta^3 R} P(f, f_{max}) \quad (2)$$

$$f_c = 49000\beta \left( \Delta\sigma/M_o \right)^{1/3} \quad (3)$$

$$P(f, f_{max}) = \frac{1}{\left[ 1 + \left( f/f_{max} \right)^c \right]^d} \quad (4)$$

where  $M_o$  is the point source seismic moment (in Nm in eq. 3),  $S(f, f_c)$  is the omega square source model (Brune [8]) with corner frequency  $f_c$  (eq. 3),  $\Delta\sigma$  is the point source stress drop (in Mpa),  $F_s$  is the amplification factor due to the free surface,  $R$  is the station-point source distance and  $\rho$  and  $\beta$  are the average density and S-wave velocity of the media. The exponential term accounts for the regional attenuation of  $Q$  which increases with the frequency as a power law of the form  $af^b$ , where  $a$  and  $b$  determine the strength of attenuation.  $P$  is the high-frequency cut-off of the point-source acceleration spectra for frequencies above  $f_{max}$ , and  $c$  and  $d$  determine the strength of high frequency decay (eq. 4).  $G(f)$  is the frequency dependent site effect, that is equal to 1 for the case of a generic seismic bedrock ground condition.

### BROADBAND ASPERITY AND ATTENUATION PARAMETERS

First of all I obtain the asperity location, area and seismic moment from an existing slip model for the target earthquake. Asperities are defined as in Somerville et. al [9]. I calculate the low frequency velocity

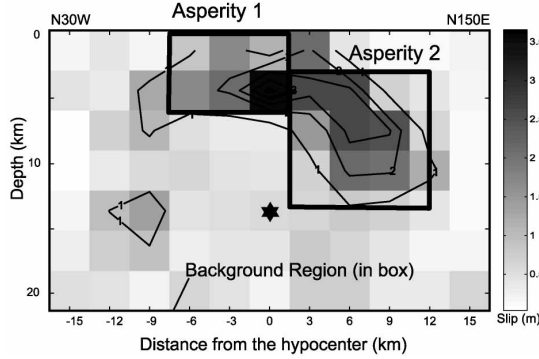


**Figure 3.** Asperity model of the 2000 Tottori earthquake. The slip model of Iwata et al. [11] is shown in grayscale.

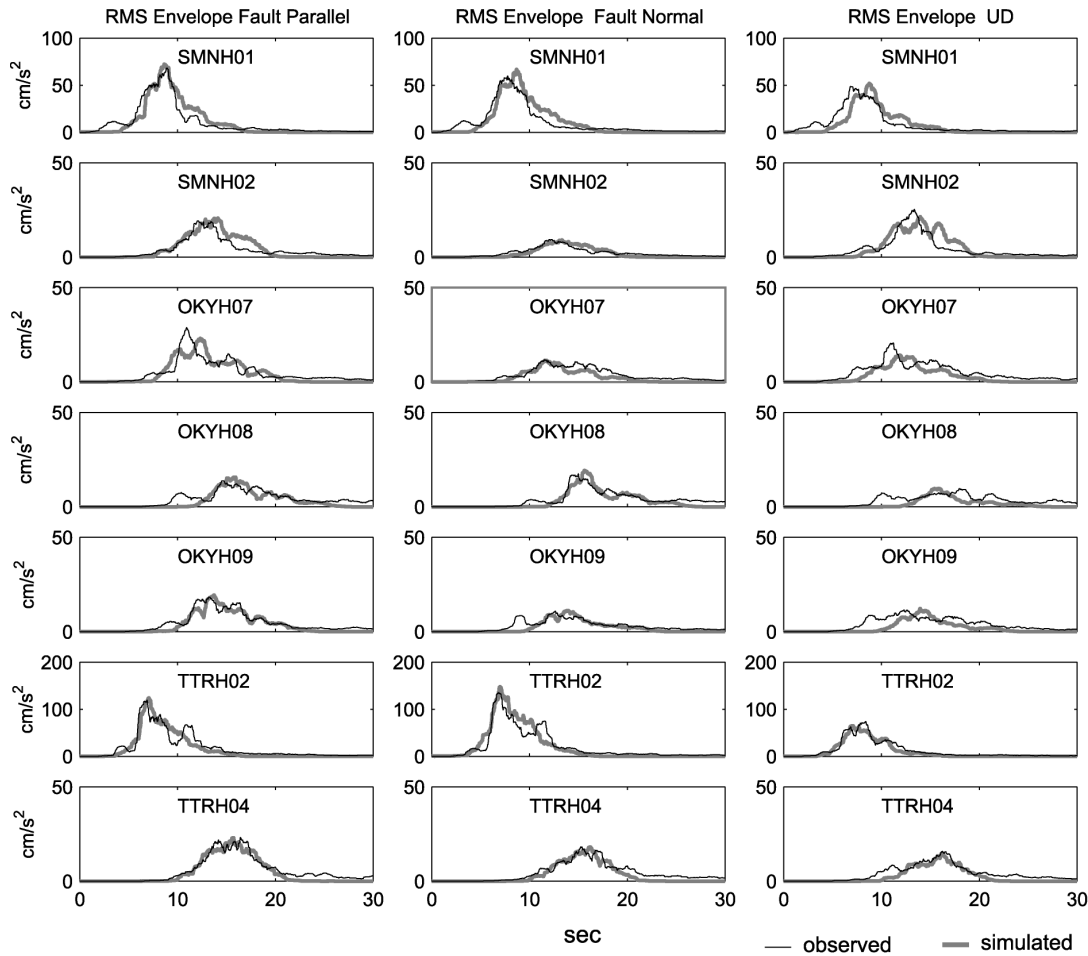


**Figure 4.** Comparison between the observed and simulated RMS acceleration envelopes (1.0 to 10Hz) during the 2000 Tottori earthquake. The envelopes start at the origin time. A running average window of 1.0s was used.

waveforms (0.1Hz to 0.5Hz or 1.0Hz) at the target sites by adjusting by trial and error the rupture velocity and rise time until a satisfactory agreement with the observed waveforms is obtained.

In the next step I calculate the high frequency (1.0 or 0.5Hz to 10 or 15Hz) waveforms for a generic seismic bedrock site. The input parameters to calculate the waveforms (model parameters for GA), are the

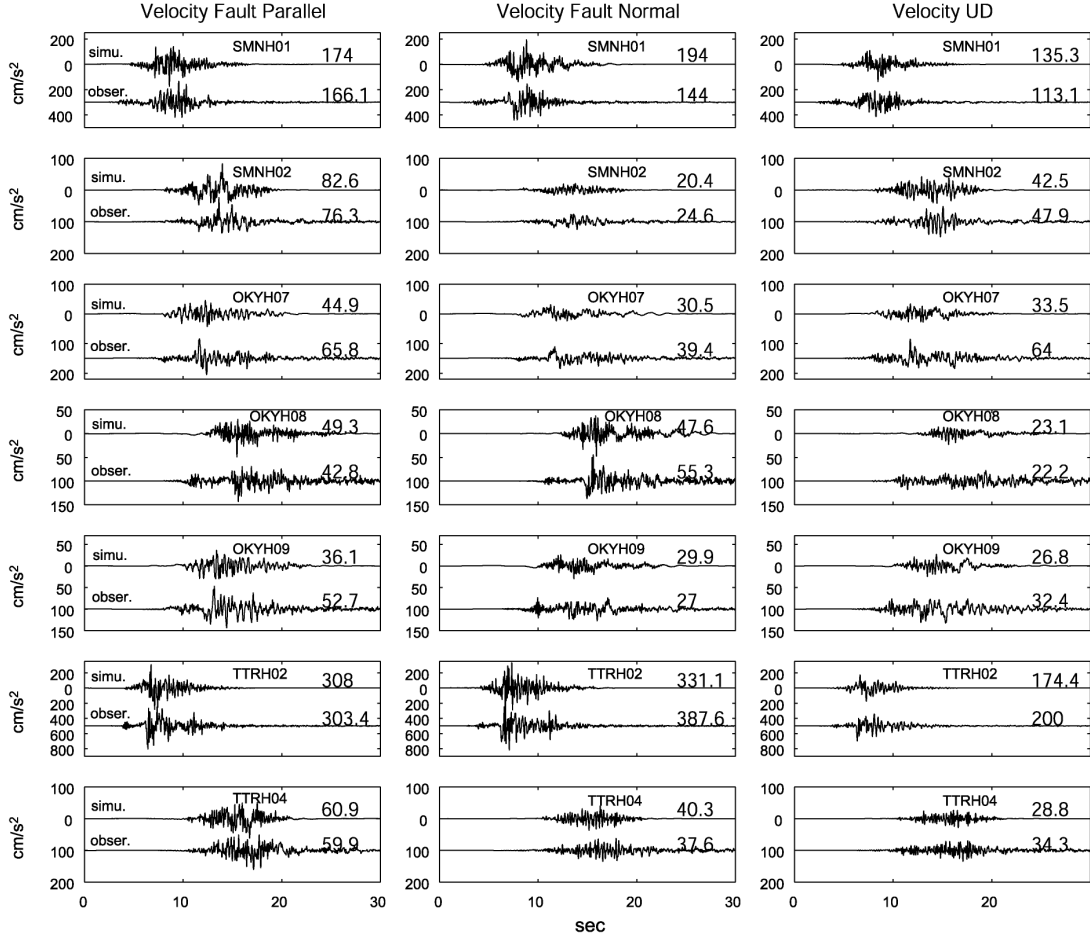


**Figure 5. Comparison between the simulated and observed broadband acceleration waveforms (0.1 to 10Hz) during the 2000 Tottori earthquake. The waveforms start at the origin time.**

stress drop of asperities and background region,  $Q(f)$ ,  $f_{max}$ , and the high frequency decay coefficients  $c$  and  $d$  (eq. 4). I use the constant rupture velocity and rise time obtained in the previous step. After that I calculate the site effects at every station, defined as the ratio between the observed acceleration response spectra (from 1 to 10 sec), to the generic-seismic-bedrock response spectra. Subsequently the high frequency waveforms are re-calculated by including the site effects and finally the RMS acceleration envelopes of simulated and observed waveforms are compared at all the stations. This step has the purpose of constraining the frequency contain of the simulated waveforms in order to bound the range of possible solutions within those that satisfy the acceleration response spectra of the observations. The process is repeated by applying a genetic algorithm inversion scheme (Houck et. al. [10]) until an optimum solution of the model parameters is obtained (Figure 1). The objective function for the inversion is as follows:

$$fit_{arms} = \frac{1}{2n} \sum_{i=1,n} \left[ 1 - \frac{\int (arms_{obs} - arms_{sim})^2 dt}{\int arms_{obs}^2 dt} \right] \quad (5)$$

where  $n$  is the total number of stations, and  $arms_{obs}$  and  $arms_{sim}$  are the observed and simulated root mean square acceleration waveforms.

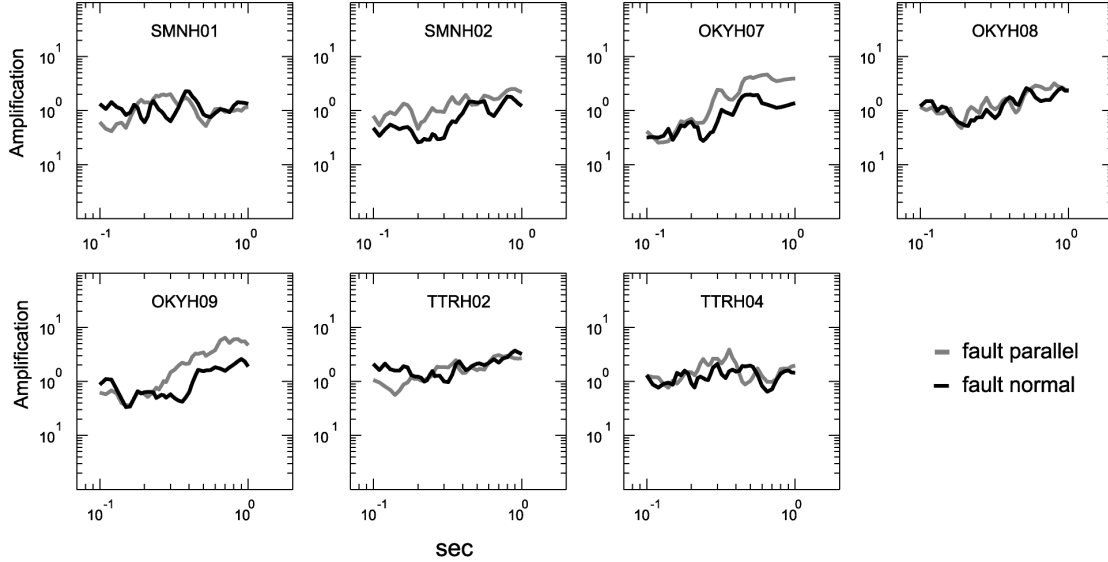


**Figure 6. Estimated site effects for the two horizontal components of the KiK-Net borehole stations used for the 2000 Tottori earthquake inversion.**

### Application to the 2000 Tottori Earthquake

The October 6/2000 Western Tottori prefecture earthquake (Japan) was an intermediate size strike-slip event that generated a large number of near-fault ground motion recordings. I simulated the ground motion at all the KiK-Net borehole stations in the near-fault region (Figure 2a). I used the records at the bottom of the boreholes, at an average depth of 100 m in order to avoid shallow site effects.

I used the slip model obtained from a kinematic inversion of near-fault ground motion (Iwata et al., [11]), to estimate the area, location and seismic moment of the asperities (Figure 3). Then I obtained the optimum rupture velocity and rise time by modeling the observed low frequency velocity waveforms. The low frequency waveforms were calculated using a flat-layered velocity structure obtained by overlapping the crustal velocity model of the Tottori region (DPRI [12]) with the KiK-Net borehole information. The modeling of the low frequency velocity waveforms yielded a rupture velocity value of 2.2 km/s for asperities 1 and 2 and the background region. The rise time is 1.6s for asperities 1 and 2 and 1.7s for the background region.

The high frequency modeling by GA (1.0 to 10Hz) produced a Q value of  $232 f^{0.71}$ , an  $f_{\max}$  value of 7Hz and high frequency decay parameters of  $c = 0.85$  and  $d = 0.6$  (eq. 4). Regarding the stress drop I obtained values of 79 bar, 150 bar and 95 bar for asperities 1, 2 and background region respectively. I obtained a very good agreement between the observed and simulated RMS acceleration envelopes (1 to 10 Hz) (Figure 4), as well as broadband acceleration waveforms (0.1 to 10 Hz) (Figure 5), for a time window of 10s from the S-wave onset. The agreement between observed and simulated acceleration response spectra was also very good demonstrating the effectiveness of the constraint during the inversion.

In Figure 6 we show the results for the estimation of site effects at the borehole sites. We can observe that despite being located at rock sites the borehole stations show a significant site effect for some stations like OKYH07 and OKYH09. We obtained that the site effects of the two horizontal components are different for these two stations suggesting the possibility of 2D site effects.

### Application to the 1999 Izmit Earthquake

We investigated the broadband asperity parameters of the 1999 Izmit (Turkey) earthquake by using 7 near-fault stations provided by the Bogazici University and the General Directorate of Disaster Affairs (Figure 2b), and following the procedure described in Figure 1.

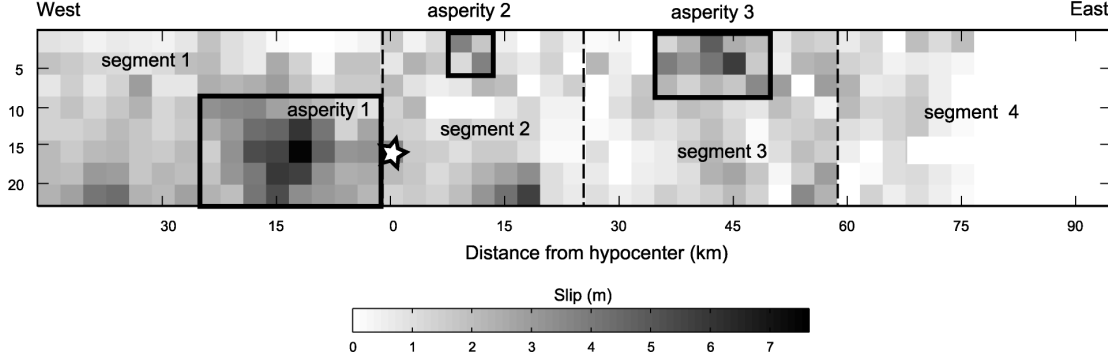


**Figure 7. Asperity model of the 1999 Izmit (Turkey) earthquake. The slip model of Sekiguchi and Iwata [13] is shown in grayscale.**

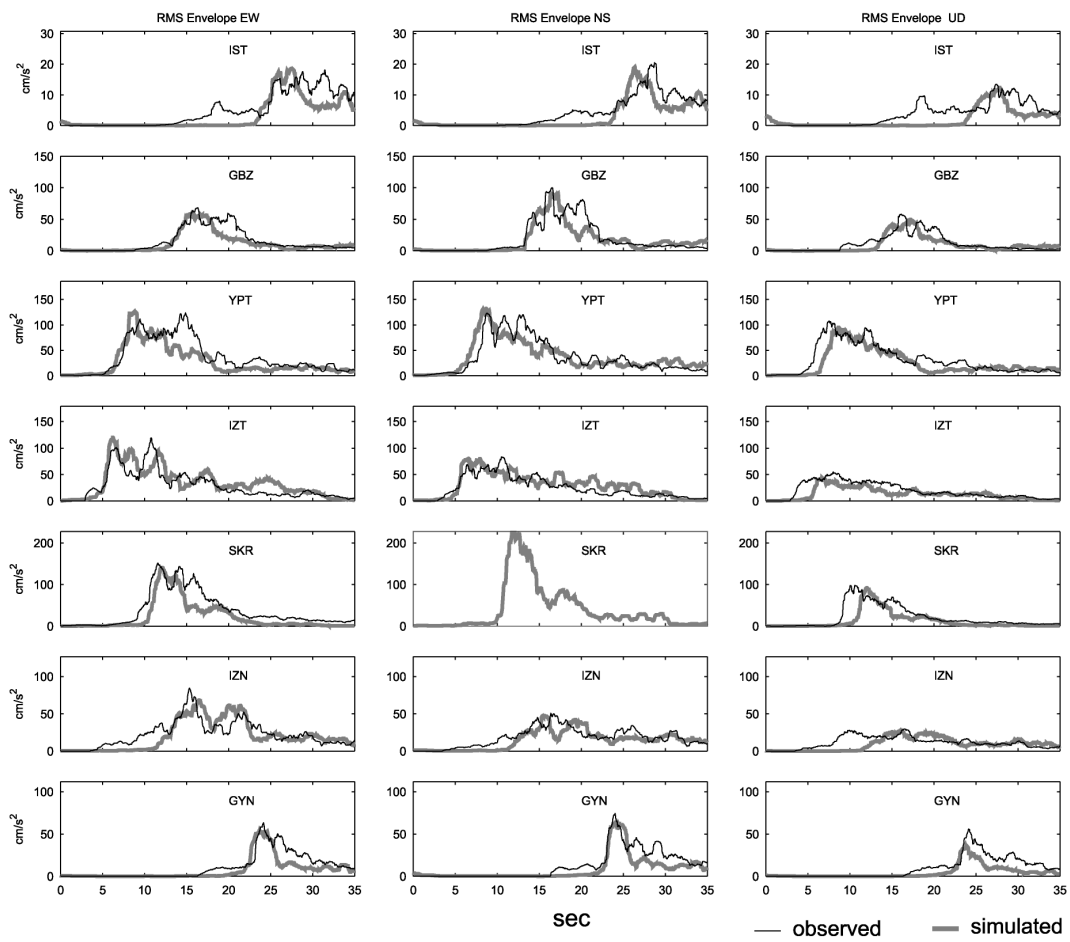


**Figure 8. Comparison between observed and simulated RMS acceleration envelopes (0.5 to 15Hz) during the 1999 Izmit earthquake. The envelopes start at the origin time. A running average window of 1.0s was used.**

The asperity area, location and seismic moment was evaluated from the slip model of Sekiguchi and Iwata [13], as shown in Figure 7. The model consists of 3 fault segments with one asperity at each segment. Segment 4 was not included in the model because of its low slip. For the calculation of the low frequency velocity waveforms I used the velocity model of Mindevalli [14] at all the stations except YPT. The velocity model at YPT was obtained by overlapping the results of Kudo [15], and Mindevalli [14]. From the modeling of the low frequency velocity waveforms I obtained a rupture velocity of 2.5 km/s and

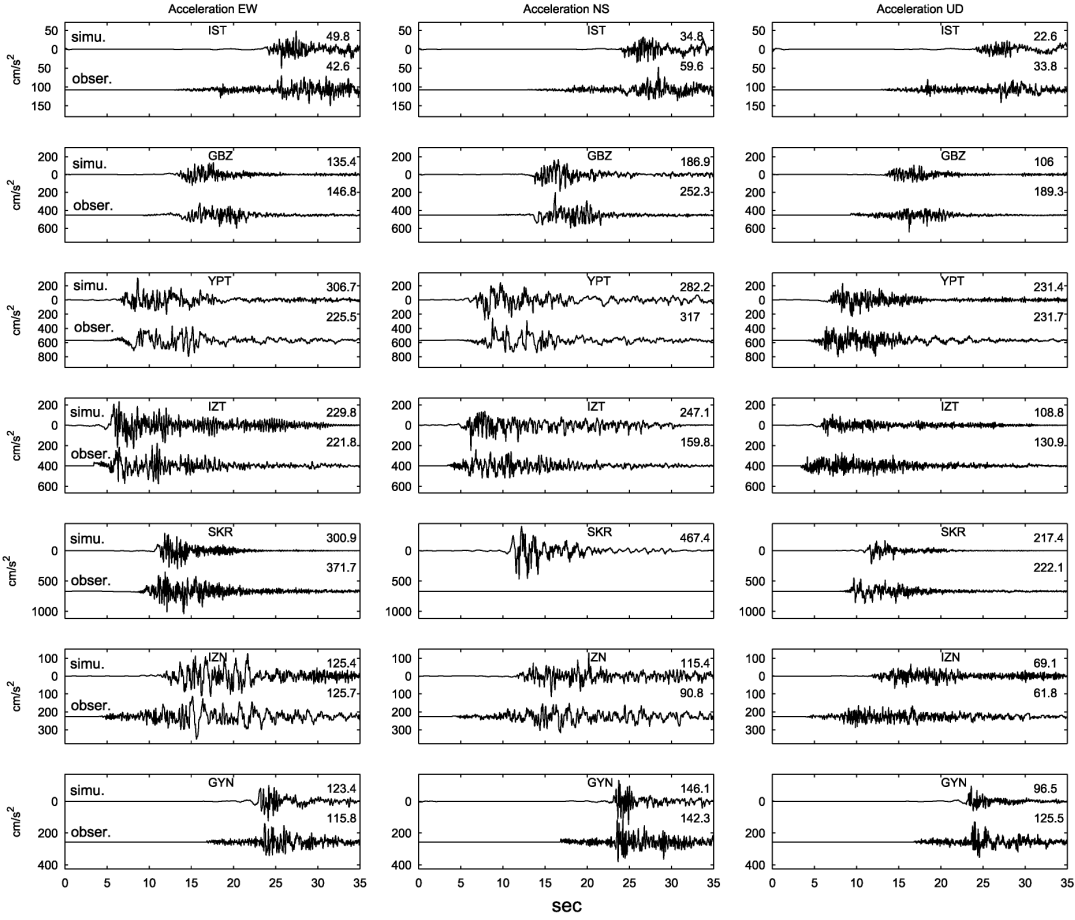


**Figure 9. Comparison between the simulated and observed broadband acceleration waveforms (0.1 to 15Hz) during the 1999 Izmit earthquake. The waveforms start at the origin time.**

3.5 km/s for asperity 1 and its background region respectively (segment 1). The rupture propagation to the west of the epicenter was set to 4.8 km/sec. Regarding the rise time I obtained a value of 2.5 s and 4.5 s for asperity 1 and its background region, and 3.0 s and 4.5 s for segments 2 and 3 respectively.

The inversion of the high frequencies (0.5Hz to 15Hz) produced a Q value of  $113.4 f^{1.2}$ , an  $f_{\max}$  value of 5.2Hz and high frequency decay parameters  $c$  and  $d$  of 7.5 and 0.47. The agreement between simulated and observed envelopes (Figure 8) and broadband acceleration waveforms (Figure 9) for a time window of 15s from the S-wave onset, are satisfactory. As before, the constraint on the simulated acceleration response spectra was very effective.

Unlike the borehole stations used for the Tottori earthquake, most of the stations used for the inversion of the asperity parameters of the Izmit earthquake are located in soil. Figure 10 shows the results for the site effects estimation at the 7 stations. In general we can observe that there is a little amplification for periods shorter than 0.3 sec, and for longer periods the sites effects are significant at all the stations. For the IST, GBZ and YPT stations there is an important difference between the site effects of the two horizontal components at periods longer than 0.3 sec (Figure 10).

### CONCLUSIVE REMARKS

I proposed a methodology for the systematic estimation of broadband frequency asperity parameters of past crustal earthquakes that adequately reproduce the observed near-fault ground motion (RMS acceleration envelopes and acceleration response spectra), by applying a Genetic Algorithm inversion scheme.

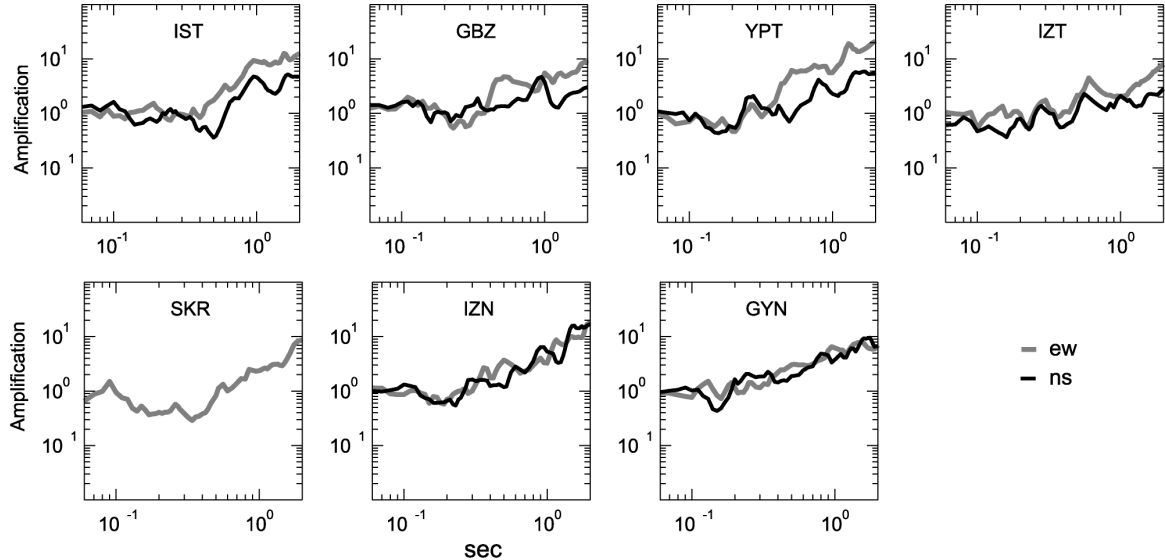


**Figure 10. Estimated site effects for the two horizontal components of the stations used for the 1999 Izmit earthquake inversion.**

The methodology was successfully applied to obtain the broadband asperity parameters of the 2000 Tottori earthquake (Japan) and 1999 Izmit earthquake (Turkey), and to simulate the near-fault ground motion. The simulation of the Tottori earthquake demonstrated that the borehole stations have an important site effect at most of the stations, despite being located in rock sites with an average S-wave velocity of 1900 m/s at the borehole depths. The inversion results for the 1999 Izmit earthquake show that all the stations have site effects for periods longer than 0.3s and the site effects are close to 1.0 for shorter periods.

The methodology presented in this paper has the potential to be used for the investigation of the high frequency radiation from the source. We have shown that the near-fault high frequency ground motion of the Tottori and Izmit earthquakes can be adequately represented by finding the appropriate values of stress drop,  $f_{\max}$  and high frequency decay values for a simple asperity model. However in order to investigate the complex high frequency radiation from the source, represented by a heterogenous stress drop across the fault plane, an effective constraint on the site effects and Q values are required. To achieve this purpose, it is desirable to first estimate the site effects and Q values from others methodologies and then investigate a heterogeneous stress drop distribution by slightly modifying the methodology described in this paper.

## REFERENCES

1. Kamae, K., K. Irikura and Y. Fukuchi, 1990. A Study of Ground Motion Prediction Procedure using Empirical Green's Function, *8<sup>th</sup> Japan Earthquake Engineering Symposium*, 223-228.
2. Kamae, K., K. Irikura and A. Pitarka, 1998. A Technique for Simulating Strong Ground Motion Using Hybrid Green's Function, *Bull. Seism. Soc. Am.* 88, No. 2, 357-367.
3. Boore, D. M., 1983. Stochastic simulation of high frequency ground motions based on seismological models of the radiation spectra, *Bull. Seism. Soc. Am.*, **73**, 1865-1894.
4. Irikura, K., 1986. Prediction of strong acceleration motion using empirical Green's function, *7<sup>th</sup> Japan. Earthq. Eng. Symp.* 151-156.
5. Pitarka A., P. Somerville, Y. Fukushima, T. Uetake and K. Irikura, 2000. Simulation of Near-Fault Strong-Ground Motion Using Hybrid Green's Function, *Bull. Seism. Soc. Am.* 90, No. 3, 566-586.
6. Pulido N., T. Kubo, 2004. Near-Fault Strong Motion Complexity of the 2000 Tottori Earthquake (Japan) from a Broadband Source Asperity Model , *Tectonophysics* (in press).

7. Bouchon, M., 1981. A simple method to calculate Green's functions for elastic layered media, *Bull. Seism. Soc. Am.*, **71**, 4, 959-971.
8. Brune, J.N., 1970. Tectonic stress and the spectra of seismic shear waves from earthquakes, *J. Geophys. Res.*, **75**, 4997-5009.
9. Somerville, P., K. Irikura, R. Graves, S. Sawada, D. Wald, N. Abrahamson, Y. Iwasaki, T. Kagawa, N. Smith and A. Kowada, 1999, Characterizing Crustal Earthquake Slip Models for the Prediction of Strong Ground Motion, *Seismological Research Letters.*, **70**, No.1, 59-80.
10. Houck, C. R., J.A. Joines and M.G. Kay, 1995. A genetic algorithm for function optimization: A Matlab implementation, *Technical Report NCSU-IETR-95-09, North Carolina State University*.
11. Iwata, T., H. Sekiguchi, Y. Matsumoto, H. Miyake, and K. Irikura, 2000. Source Process of the 2000 Western Tottori Prefecture Earthquake and Near-Source Strong Ground Motions, *Fall Meeting of the Seismological Society of Japan*.
12. DPRI, 2000. Crustal velocity Structure of the Tottori region (personal communication). Disaster Prevention Research Institute (DPRI), Kyoto University.
13. Sekiguchi, H. and T. Iwata, 2002. Rupture Process of the 1999 Kocaeli, Turkey, Earthquake Estimated from Strong-Motion Waveforms, *Bull. Seism. Soc. Am.*, **92**, 1, 300-311.
14. Mindevalli O., and B. Mitchell, 1989, Crustal structure and possible anisotropy in Turkey from seismic surface wave dispersion, *Geophys. J. Int.*, **98**, 93-106.
15. Kudo, K., T. Kanno, H. Okada, O. Ozel, M. Erdik, T. Sasatani, S. Higashi, M. Takahashi, and K. Yoshida, 2002, Site-Specific Issues for Strong Ground Motions during the Kocaeli, Turkey, Earthquake of 17 August 1999, as Inferred from Array Observations of Microtremors and Aftershocks, *Bull. Seism. Soc. Am.*, **92**, 1, 448-465.